Coupling of surface plasmons in nanostructured metal/dielectric multilayers with subwavelength hole arrays

Z. H. Tang, R. W. Peng,* Z. Wang, X. Wu, Y. J. Bao, Q. J. Wang, Z. J. Zhang, W. H. Sun, and Mu Wang
National Laboratory of Solid State Microstructures and Department of Physics, Nanjing University, Nanjing 210093, China
(Received 2 April 2007; revised manuscript received 11 August 2007; published 6 November 2007)

We demonstrate here that the enhancement of optical transmission originates not only from surface plasmons (SPs) but also from the coupling of SPs in the Ag/SiO_2 multilayer with a periodic array of subwavelength holes. The multilayer film is constructed by repeating a building block, which contains two layers: one is a silver film with periodic array of subwavelength holes and the other is a film of SiO_2. The multilayers were fabricated by magnetron sputtering, and the array of holes was milled with focused-ion-beam facility. The measured optical transmission properties reasonably agree with our numerical calculations. It is shown that the coupling of SPs strongly depends on the detailed structure, and in our system, the coupled SPs can be characterized by using an effective-permittivity model. In the sandwiched structure with nanostructured silver, the coupling of SPs leads to the shift of transmission peaks, while in a nanostructured Ag/SiO_2 multilayer, the coupling of SPs yields a new resonant mode with increased quality factor of the transmission peak, which originates from multiple scatterings and the coupling of electromagnetic waves on the interfaces of the multilayers. These properties may be utilized to tune electromagnetic wave in subwavelength optics.

DOI: 10.1103/PhysRevB.76.195405 PACS number(s): 78.67.−n, 42.25.Bs, 78.68.+m

I. INTRODUCTION

When electromagnetic wave irradiates on a metal surface, driven by the high frequency electric field, free electrons on the metal surface may oscillate accordingly. The interaction between the surface charge oscillation and the electromagnetic field of the light generates a surface wave known as surface plasmon (SP). Usually, this kind of elementary excitation in the system is also termed as surface plasmon polariton (SPP). In 1957, Ritchie[1] predicted the existence of SPs when he discussed the plasma losses by fast electrons in thin films. Recently, some fascinating issues have added fresh insight into the subject of SP. First, in 1998, Ebbesen *et al.*[2] reported the extraordinary optical transmission (EOT) through a two-dimensional array of subwavelength holes perforated on silver film. It is found that the EOT in the subwavelength holes originates from the SP in resonance with the lattice structure.[2–4] Second, SPs can be tailored by adjusting the subwavelength structures on metal surface, including altering the type and the thickness of metal and the size and geometry of the holes.[5–11] Nowadays, it is possible to design various kinds of structures, in which SPs can be excited and tuned. In this way, novel materials and potential devices can be realized,[12] such as the left-handed materials[13,14] and imaging of superlens and hyperlens.[15] Third, the SP-based circuits can merge photonics and electronics on nanoscale, which offers the potential applications including plasmonic chips, nanolithography, and biophotonics.[16]

It is well known that at the interface separating a metal and a dielectric, the SP mode obeys the following dispersion relation:

$$k_{sp} = k_0 \sqrt{\frac{\varepsilon_d \varepsilon_m}{\varepsilon_d + \varepsilon_m}}, \tag{1}$$

where k_0 is the wave vector of the incident light and ε_m and ε_d are the permittivities of the metal and the dielectric, respectively. In the metal film with periodic array of subwavelength holes and sandwiched by two dielectric media, two kinds of SP dispersion curves on top and bottom interfaces may translate by multiple reciprocal lattice vectors of the hole array. Then, there might be some crossovers between two kinds of SP dispersion curves. At those crossovers, the coupling of SPs[17] will take the form of evanescent wave. Usually, the coupling of SPs leads to a band gap in the band structure of SPs,[4] which originates from the periodicity in an infinite structure. However, in a finite system, the coupling of SPs may generate even richer features. Now, the following question arises: Is it possible to design a system in which the coupling of SPs can be intentionally tuned so that the transmission can be effectively adjusted? By doing so, the basic processes involved in the excitation and coupling of SPs become clearer, and potentials to apply SP-based effects become more evident. With this purpose, we report in this paper our investigations on the coupling of SPs in Ag/SiO_2 multilayers with a periodic array of subwavelength holes. It is shown that the main peaks in the measured transmission spectrum have been indexed by using effective-permittivity model, and the coupling of SPs in the nanostructured Ag/SiO_2 multilayer can yield a new resonant mode. The quality factor of the transmission peak can be increased with increasing the number of building blocks. These features originate from multiple scatterings and the coupling of electromagnetic waves on the interfaces of the multilayers. The optical measurements reasonably agree with numerical calculations based on the full-vectorial three-dimensional finite-difference time-domain (FDTD) method.

In this paper, we start from the coupling of SPs in several sandwiches with nanostructured silver (shown in Sec. II). Then, we study the coupling effect of SPs on the optical transmission in the nanostructured Ag/SiO_2 multilayer (shown in Sec. III). Finally, a summary is given in Sec. IV.

II. COUPLING OF SURFACE PLASMONS IN THE SANDWICH STRUCTURE

We study the optical properties of silver film perforated with periodic array of subwavelength holes in following three environments. (i) The silver film is freestanding and the holes are in vacuum. This scenario is denoted as A-Ag-A. (ii) The silver film is sandwiched by silicon oxide, and the holes are filled with silicon oxide. This scenario is denoted as Q-Ag-Q. (iii) The silver film is sandwiched between vacuum and silicon oxide, and the holes are in vacuum. This scenario is termed as A-Ag-Q. The thickness of silver film, the periodicity of the holes in the array, and the size of the holes are the same for each case. We first carry out computer simulations based on the full-vectorial three-dimensional FDTD method.[18] The frequency-dependent permittivity of silver is based on the Lorentz-Drude model,[19] and the permittivity of silicon oxide is taken as $\varepsilon_{SiO_2}=2.16$. Periodic boundary condition is applied for in-plane boundaries, and perfectly matched layer is set for the perpendicular boundary. The grid spacing is carefully chosen to guarantee convergence in the calculation. The transmission and the reflection of electromagnetic waves through each film have been calculated. In this work, we focus on normal incidence only. Figures 1(a)–1(c) show the transmission and reflection spectra of the films of A-Ag-A, Q-Ag-Q, and Ag-Ag-Q, respectively. For each scenario, the thickness of silver film is $t_{Ag}=100$ nm, the separation of the holes (spatial periodicity) is $a_0=600$ nm, and the diameter of the holes is $d=150$ nm. The maxima in transmission spectra and the minima in reflection spectra can be clearly identified. The transmission peaks of the A-Ag-A film are located at the range of wavelength from 400 to 750 nm [as shown in Fig. 1(a)], while the transmission peaks of the Q-Ag-Q film and the A-Ag-Q film appear in the range from 400 to 1050 nm [as shown in Figs. 1(b) and 1(c)]. The transmission peaks in the A-Ag-Q film are much denser compared to the scenarios of A-Ag-A and Q-Ag-Q.

It is well established that the enhancement of transmission is due to light coupling with SPs in the metallic-dielectric surface. In the metal film with a periodic array of holes, the interaction between light and the SP obeys momentum conservation,[2]

$$\vec{k}_{sp} = \vec{k}_0 \sin\theta + (i\vec{G}_x + j\vec{G}_y), \tag{2}$$

where $\vec{k}_{sp}$ is the wave vector of the SP, $\vec{k}_0 \sin\theta$ is the in-plane component of the incident wave vector, $\vec{G}_x$ and $\vec{G}_y$ are the reciprocal lattice vectors with the same value as $|\vec{G}_x|=|\vec{G}_y|=2\pi/a_0$, and i,j are both integers. On the other hand, there may exist coupling of SPs in the structured metal/dielectric system, and also other excitations therein, such as the excitation of cavity plasmon-polaritons.[20] (We will show that the excitation of cavity plasmon-polaritons is weak in our system.) In order to describe the dispersion relation of SPs in these systems, we use an effective permittivity ε_{eff} of the structured metal instead of the previous permittivity ε_m of the metal. Here, we assume that the light through the structured metal film can be effectively considered as that through a uniform metal with ε_{eff}, and both cases have identical optical transmission and reflection on the planar film. Thereafter, the SP dispersion relation at the metallodielectric interface can be rewritten as

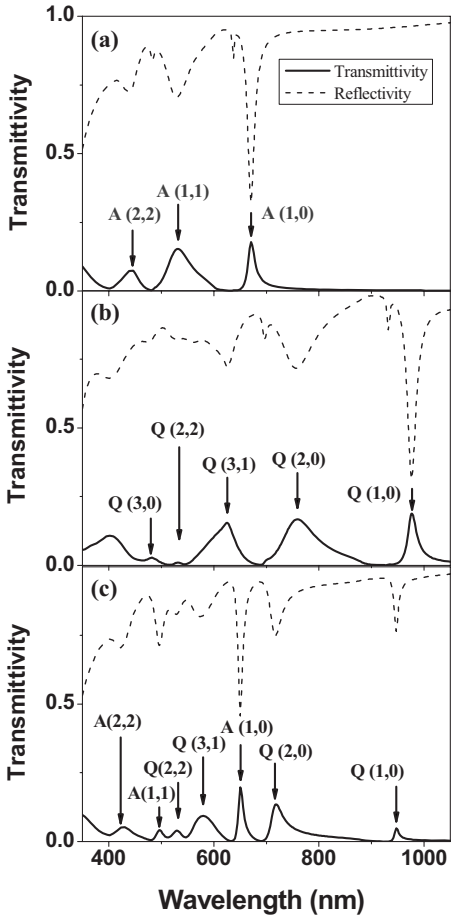

FIG. 1. The calculated transmission and reflection spectra of the structured silver films when the incident beam is perpendicular to the film. (a) A-Ag-A, where the silver film is freestanding and holes are in vacuum. (b) Q-Ag-Q, where the silver film is sandwiched by silicon oxide films and holes are filled also with silicon oxide. (c) A-Ag-Q, where the silver film is sandwiched between vacuum and silicon oxide and holes are in vacuum. In each film, the thickness of silver is 100 nm, the period of hole array is 600 nm, and the diameter of hole is 150 nm. In the calculation, the computational domain size is set as 0.6 μm for in-plane and 2 μm for the depth, respectively. The grid spacing is set as $7.5\times7.5\times5$ nm^3. The main peaks are indexed as described in the text.

$$k_{sp} = k_0\sqrt{\frac{\varepsilon_d\varepsilon_{eff}}{\varepsilon_d+\varepsilon_{eff}}}. \tag{3}$$

Considering Eqs. (2) and (3) in the case of normal incidence $\theta=0$, we can obtain the maximum transmission satisfying

$$\lambda_{max} = \frac{a_0}{\sqrt{i^2+j^2}}\sqrt{\frac{\varepsilon_d\varepsilon_{eff}}{\varepsilon_d+\varepsilon_{eff}}}. \tag{4}$$

Therefore, the transmission peaks can be indexed with integers (i,j) in the optical spectra. The effective permittivity of

the structured metal ε_{eff} can be derived from the reflectivity and transmittivity of light in the metallodielectric system. Basically, the effective permittivity presented here is similar to that in the Maxwell-Garnett effective-medium theory.[21] The former focuses more on the equivalent optical properties, whereas the latter follows the exact volume fraction of each medium in the structure.

In the A-Ag-A film, main transmission peaks can be indexed as $A(1,0)$ at 671 nm, $A(1,1)$ at 532 nm, and $A(2,2)$ at 443 nm [as shown in Fig. 1(a)], which originate from the SP at the interface of air-silver and A stands for SP at the air-silver interface. In the Q-Ag-Q film, the transmission peaks come from the SP at the SiO_2-silver interface. The main transmission peaks can be indexed as $Q(1,0)$ at 977 nm, $Q(2,0)$ at 760 nm, $Q(3,1)$ at 625 nm, respectively [as shown in Fig. 1(b)]. Here, Q denotes the SP at the SiO_2-silver interface. For the film of A-Ag-Q, there are two kinds of SPs on the air-silver interface and the SiO_2-silver interface, respectively. The coexistence of SPs on the two interfaces can be identified in the transmission spectrum of the A-Ag-Q film [as shown in Fig. 1(c)]. For example, there are modes indexed by $A(1,0)$, $A(1,1)$, $Q(1,0)$, $Q(2,0)$, and $Q(3,1)$. The main resonant modes in both A-Ag-A and Q-Ag-Q films indeed appear in the transmission spectrum of the A-Ag-Q film [as shown in Fig. 1(c)].

It is interesting that SP on one surface of Ag film can couple with that on the other surface. If the SP of the same mode exists on both surfaces of Ag film, the coupling of SPs leads to the enhancement of the transmission. For example, the peak indexed by $Q(1,0)$ in Q-Ag-Q film [as shown in Fig. 1(b)] is obviously higher than that in the A-Ag-Q film [as shown in Fig. 1(c)]. If, however, SPs of different modes exist on each sides of the silver film, we find that the coupling of SPs leads to a blueshift of the transmission modes. For example, the mode $A(1,0)$ in the A-Ag-A film is located at 671 nm [as shown in Fig. 1(a)], which shifts to 650 nm in the A-Ag-Q film [as shown in Fig. 1(c)]. The mode $Q(2,0)$ in the Q-Ag-Q film is located at 760 nm [as shown in Fig. 1(b)], which shifts to 719 nm in the A-Ag-Q film [as shown in Fig. 1(c)]. Furthermore, due to the fact that coupling of SPs is influenced by the thickness of metallic film, the blueshift of the transmission peak depends on the thickness of the metallic film. Figure 2 shows the blueshift of several transmission modes as a function of the thickness of Ag film in the A-Ag-Q system. It is obvious that the blueshift of the transmission peaks decreases exponentially with increasing the thickness of the Ag film (as shown in Fig. 2). These features make it possible to tune the transmission peak by adjusting the coupling of SPs at different metallic-dielectric interfaces.

In order to understand the basic physical processes involved in the generation of SPs and their coupling in the structure, we calculate the density distribution of the electric field of several modes in the sandwiched structures. The cross-sectional profile of the density distribution is shown in Fig. 3, and the in-plane profile is illustrated in Fig. 4. For mode $A(1,0)$, when the p-polarized light illuminates the A-Ag-A film from top to bottom [as shown in Fig. 3(A1)], the SP appears on the top surface and is enhanced [as shown in Fig. 3(A2)]. Then, the SP is generated on the bottom surface and coupled with the SP on the top surface [as shown in Fig. 3(A3)]. Gradually, SP on the top surface is weakened, while the SP on the bottom surface is enhanced. As a result, their coupling diminishes, as shown in Figs. 3(A4)–3(A6), while for the same mode $A(1,0)$ in A-Ag-Q film, SP appears mainly on the top surface (air-silver interface) and is enhanced [as shown in Figs. 3(B2)–3(B4)]. Gradually, SP on the top surface is affected by the electromagnetic wave on the bottom surface and is weakened, as shown in Figs. 3(B4)–3(B6). As time goes on, these physical processes repeat periodically. Therefore, electromagnetic waves on the top surface and on the bottom surface are indeed coupled. What happens on the in-plane is the following. The maximum density distribution of the electric field of mode $A(1,0)$ is illustrated in Figs. 4(a) and 4(b). Within one temporal period, there is a maximum distribution on the bottom surface of the A-Ag-A film [as shown in Fig. 4(a)], and the same mode occurs for the A-Ag-Q film [as shown in Fig. 4(b)]. Obviously, the electric field is concentrated on the edge of the hole. For the mode $Q(1,0)$, the density distribution of electric field is also investigated. Similar results are obtained. Figures 3(C1)–3(C6) show the cross-sectional density distribution in A-Ag-Q film, and Figs. 3(D1)–3(D6) show the cross-sectional density distribution in Q-Ag-Q film. The in-plane density distribution of these two structures are shown in Figs. 4(c) and 4(d), respectively. Based on these results, we conclude that the transmission optical enhancement originates not only from surface plasmons (SPs) but also from the coupling of SPs in the sandwich structure. In addition, the excitation of cavity plasmon-polaritons[20] is very weak in these systems (as shown in Figs. 3 and 4).

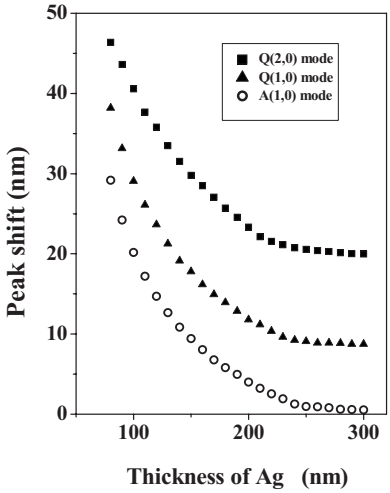

FIG. 2. The plot showing the blueshift of several transmission modes in film of A-Ag-Q as a function of the thickness of the silver film, compared to those in the film of Q-Ag-Q. In each film, the lattice parameter of the hole array is 600 nm, and the diameter of hole is 150 nm.

Experiments have been carried to verify the calculated results. The Q-Ag-Q and A-Ag-Q films have been fabricated in the following way. Firstly, silver films with the thickness of 100 nm were coated on the substrate of $K9$ optical glass by magnetron sputtering technique. Focused-ion-beam facil-

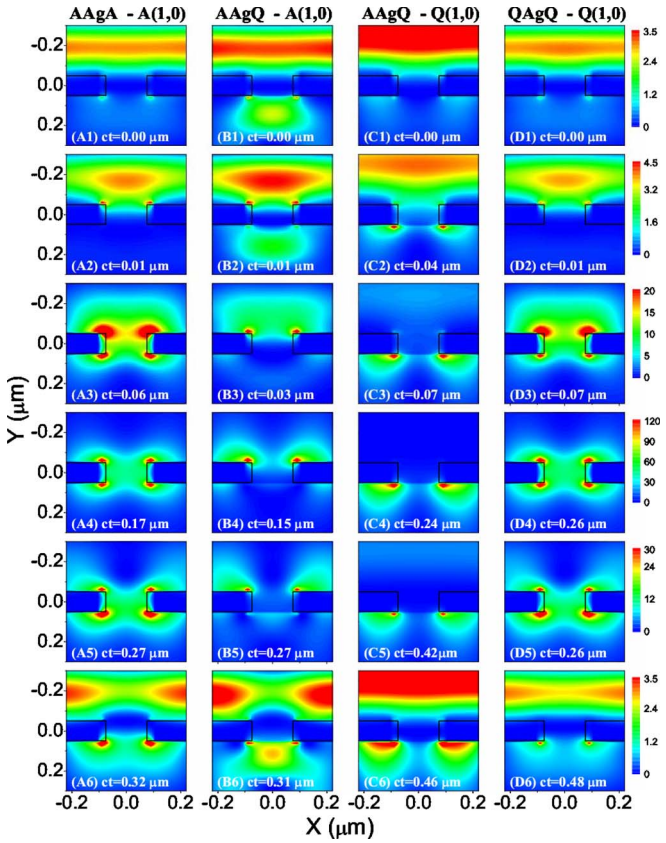

FIG. 3. (Color online) The calculated density distribution of electric field of several modes in the cross section of the sandwiched multilayer, where a *p*-polarized incident light illuminates the sandwiched film from top to bottom. Within one temporal period, the density distributions of electric field of mode $A(1,0)$ are shown in (A1)–(A6) for the sandwiched structure A-Ag-A, and (B1)–(B6) are for the sandwiched structure A-Ag-Q. For the mode $Q(1,0)$, the density distributions of the electric field are shown in (C1)–(C6) for the sandwiched structure A-Ag-Q, and (D1)–(D6) are for Q-Ag-Q. Here, c is the velocity of light in vacuum, and t is the time within a temporal period.

ity (strata FIB 201, FEI company, 30 keV Ga ions) is used to mill the array of holes on the silver film. In this way, the A-Ag-Q films were obtained. Following the same process, if a sufficiently thick layer of silicon oxide was coated on the A-Ag-Q film afterward by magnetron sputtering, a Q-Ag-Q film was formed. Field-emission scanning-electron microscope and atomic-force microscope (AFM) measurements [Figs. 5(a)–5(d)] indicate that the samples were well fabricated as designed, the period of the holes in the array was about $a_0=600$ nm, and the diameter of the hole was about $d=150$ nm for both A-Ag-Q and Q-Ag-Q films.

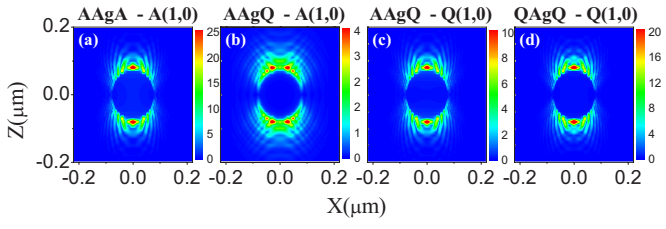

FIG. 4. (Color online) The maxima in the in-plane density distribution of electric field of two modes in the sandwiched structure. For mode $A(1,0)$ (a) in the sandwich A-Ag-A and (b) in the sandwich A-Ag-Q. For mode $Q(1,0)$ (c) in the sandwich A-Ag-Q and (d) in the sandwich Q-Ag-Q.

Optical transmission of the structured silver films has been measured by PerkinElmer Lambda 900 spectrophotometer in the range from 400 to 2500 nm when the incident beam is perpendicular to the film. Figure 6 shows the optical transmission spectra of A-Ag-Q and Q-Ag-Q films, respectively. Obviously, the main transmission peaks in the film of Q-Ag-Q can be indexed [as shown in Fig. 6(a)] as $Q(1,0)$, $Q(2,0)$, $Q(3,1)$, and $Q(3,0)$. Extraordinary optical transmission comes from the SP at the SiO_2-Ag interface, while main transmission peaks in the film of A-Ag-Q can be indexed as $Q(1,0)$, $Q(2,0)$, $A(1,0)$, $Q(3,1)$, and $Q(3,0)$, respectively [as shown in Fig. 6(b)]. Extraordinary optical transmission comes from SPs on both SiO_2-Ag and air-Ag interfaces. The coupling of SPs at these two interfaces leads to blueshift of the mode [as shown in Figs. 6(a) and 6(b)]. For example, compared to that in Q-Ag-Q film, the peak of $Q(1,0)$ in A-Ag-Q film has been blueshifted for about 17 nm, and the peak of $Q(2,0)$ in A-Ag-Q film has been blueshifted for about 27 nm. The derivation of transmission peaks between experiments and calculations is within 1%. The measured spectra are also in good agreement with the numerical calculations shown in Figs. 1(b) and 1(c). Therefore, extraordinary optical transmission in the film of A-Ag-Q comes from the SPs and their coupling on both SiO_2-Ag and air-Ag interfaces, and the coupling of SPs is responsible for the blueshift of transmission peaks. Besides, the peak intensity of $Q(1,0)$ in Q-Ag-Q [as shown in Fig. 6(a)] is much higher than that in A-Ag-Q [as shown in Fig. 6(b)]. This means that once the SP with the same mode is excited on the both sides of the Ag film, the coupling of SPs leads to the enhancement in transmission. In addition, antiresonances induced by Fano interference[22] are also observed in this system, where a characteristic dip appears in the transmission spectrum, as marked in Figs. 6(a) and 6(b). Usually, the formation of the dip can be explained as the result of destructive interference of surface modes.[23]

III. COUPLING OF SURFACE PLASMONS IN THE MULTILAYERS

The nanostructured metal/dielectric multilayer film is constructed in the following way. First, the building block of the multilayer is defined. It contains two layers: one is a silver film with periodic array of subwavelength SiO_2 holes and the other is a film of SiO_2. Then, by repeating the building block, a nanostructured Ag/SiO_2 multilayer film is obtained, as schematically shown in Fig. 7. As an example, we study several multilayer films with different repeating numbers of building block. In each building block, the thickness of silver film is $t_{Ag}=50$ nm, the lattice parameter of the hole array is $a_0=600$ nm, and the diameter of the holes is $d=150$ nm, and the SiO_2 layer has the thickness of $t_{SiO_2}=50$ nm. The repeating number of building blocks can be $n=1$, 2, 3, and 4, respectively. Figure 8 shows the calculated spectra of optical

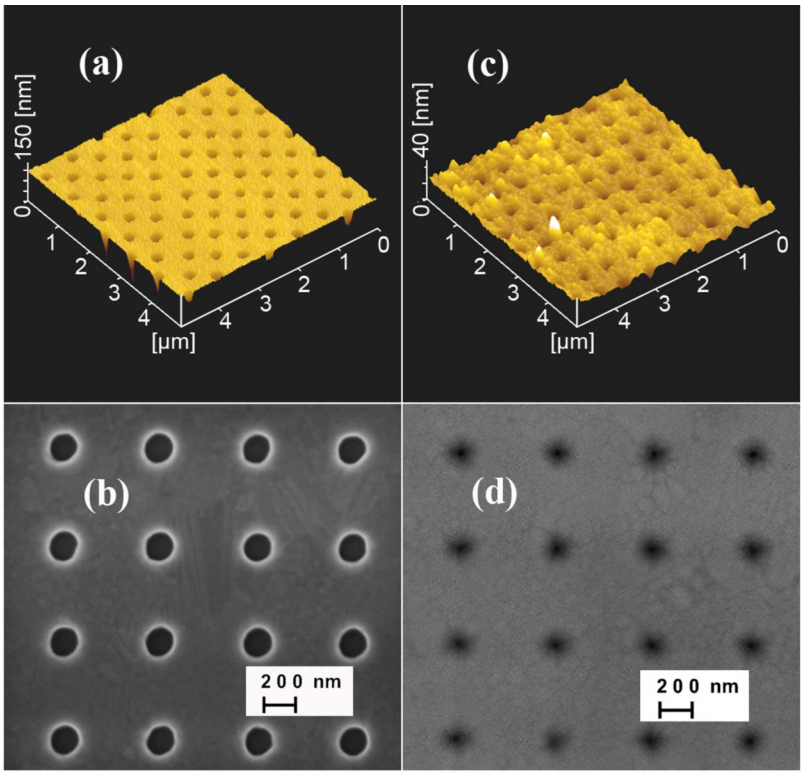

FIG. 5. (Color online) The atomic-force microscope (AFM) images of silver films perforated with a periodic array of subwavelength holes for (a) A-Ag-Q and (c) Q-Ag-Q. The scanning-electron microscope images of the same sample for (b) A-Ag-Q and (d) Q-Ag-Q.

transmission through these multilayer films based on FDTD method. It is obvious that there are indeed several transmission peaks in each spectrum. Main peaks can be indexed by two integers [as shown in Figs. 8(a)–8(d)]. Besides, there are two interesting features. First, by increasing the repeating number of building blocks, a new resonant mode appear in the transmission spectra [as shown in Figs. 8(a)–8(d)]. For example, the resonant peak labeled by $Q(3,1)$ in Fig. 8(d) does not appear when there is only one building block in the film [as shown in Fig. 8(a)]. By increasing the number of building blocks, the transmission intensity at the resonant mode $Q(3,1)$ increases gradually [as shown in Figs. 8(b) and 8(c)]. Finally, the transmission peak comes out apparently when there are four building blocks in the film [as shown in Fig. 8(d)]. Second, the quality factor of the transmission peak increases when the number of building blocks is in-

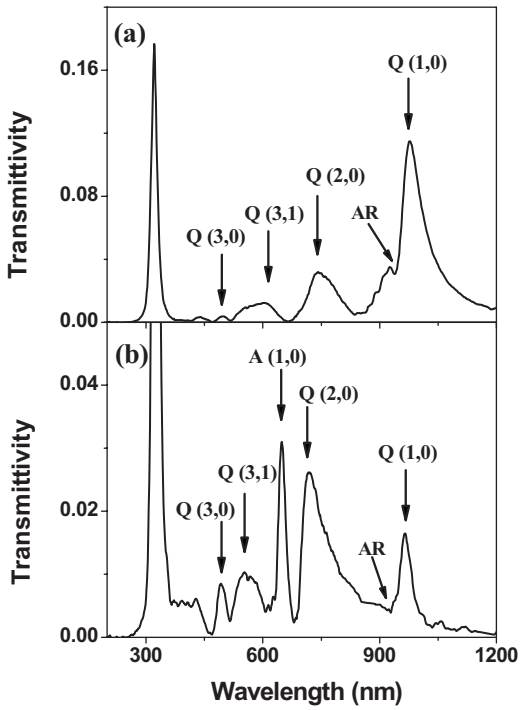

FIG. 6. The measured normalized-to-area transmittivity of structured silver films when the incident beam is perpendicular to the film for (a) Q-Ag-Q and (b) A-Ag-Q. In each film, the thickness of silver is 100 nm, the period of hole array is 600 nm, and the diameter of hole is 150 nm. The main peaks are indexed and the dips marked by "AR" are described in the text.

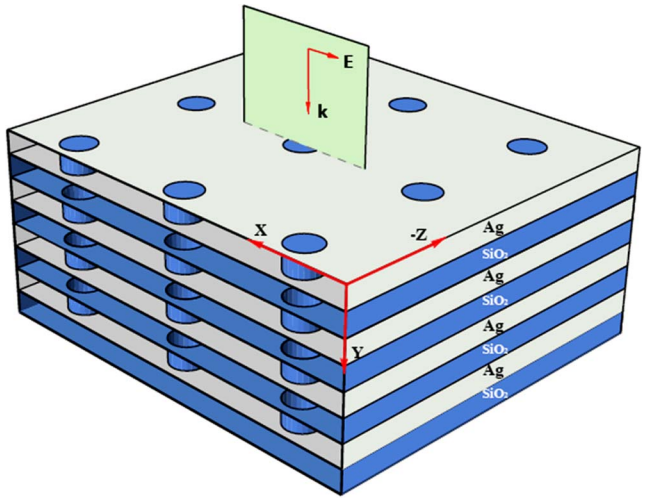

FIG. 7. (Color online) A schematic diagram for a nanostructured Ag/SiO_2 multilayer film.

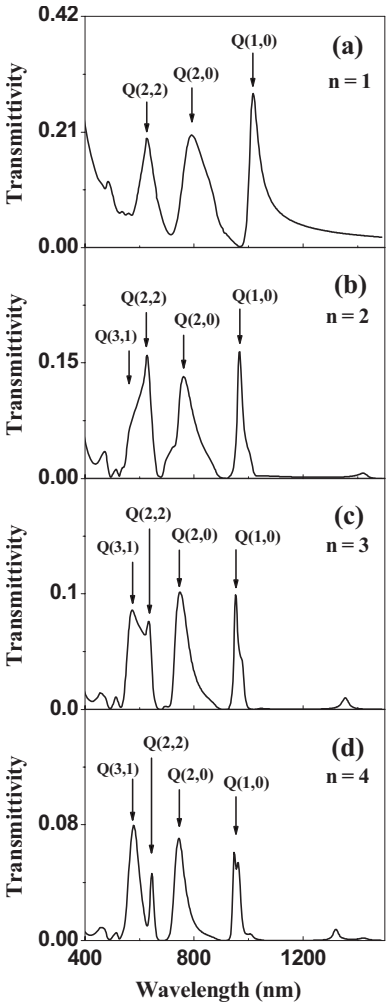

FIG. 8. The calculated transmission spectra of the nanostructured Ag/SiO_2 multilayer films with different repeating numbers of building blocks n and different total thicknesses of the film D_{tot}: (a) $n=1$ and $D_{tot}=100$ nm, (b) $n=2$ and $D_{tot}=200$ nm, (c) $n=3$ and $D_{tot}=300$ nm, and (d) $n=4$ and $D_{tot}=400$ nm, respectively. Each building block contains two layers: one is the SiO_2 layer with the thickness of $t_{SiO_2}=50$ nm and the other is silver film with the thickness $t_{Ag}=50$ nm, which is perforated with a periodic array of subwavelength hole. The spatial periodicity of the holes is $a_0=600$ nm, and the diameter of the holes is $d=150$ nm. Here, the incident beam is perpendicular to the film.

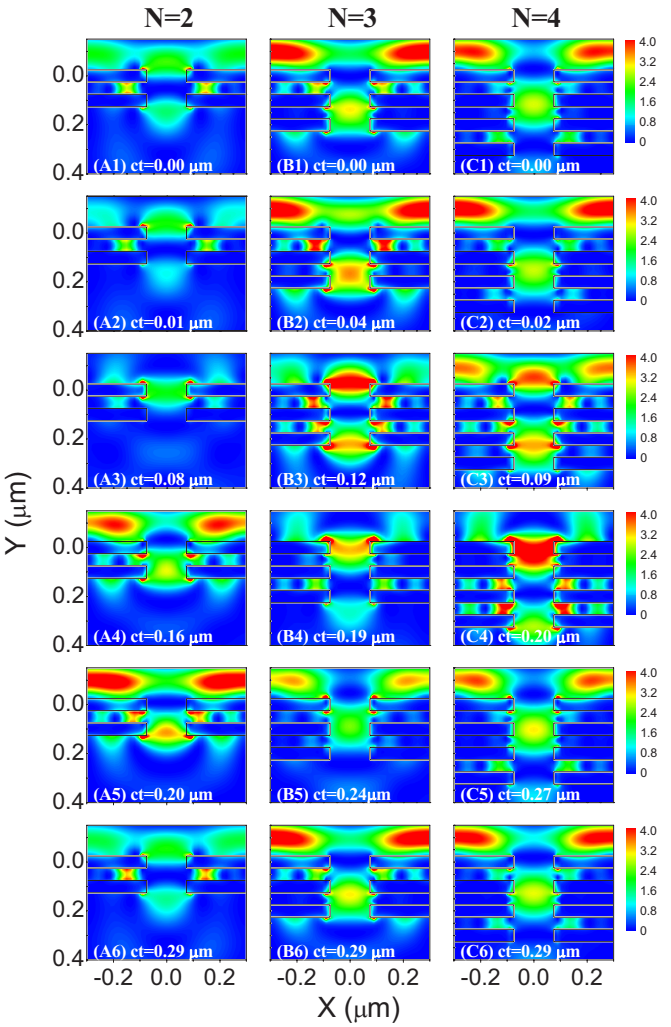

FIG. 9. (Color online) The calculated density distribution of electric field of mode $Q(3,1)$ in several multilayer films, where a p-polarized incident light illuminates the multilayer film from top to bottom. Within one temporal period, the density distributions of electric field of mode $Q(3,1)$ are shown: (A1)–(A6) in the multilayer with $n=2$, (B1)–(B6) in the multilayer with $n=3$, and (C1)–(C6) in the multilayer with $n=4$, respectively. Here, n is the repeating number of building blocks in the nanostructured Ag/SiO_2 multilayer films described in Fig. 8, c is the velocity of light in vacuum, and t is the time within a temporal period.

creased. Here, the quality factor of peak is defined as $Q=\lambda_0/\Delta\lambda$, and λ_0 is the wavelength of the peak and $\Delta\lambda$ is the half-width of the peak, respectively. As indicated in Fig. 8, the peak labeled by $Q(2,0)$ has the quality factor $Q=7.1$ for $n=1$, whereas $Q=13.1$ for $n=3$. Yet the intensity of transmission peak decreases when the number of silver layer is increased due to the absorption of silver. These features may originate from multiple scatterings and the coupling of electromagnetic waves in the multilayer film.

In order to show multiple scatterings of electromagnetic wave and also the coupling effect in the multilayer structure, we calculated the density distribution of electric field of mode $Q(3,1)$ in several multilayer films, as shown in Fig. 9. When the p-polarized incident light illuminates these films from top to bottom [as shown in Figs. 9(A1), 9(B1), and 9(C1)], the SPs will be generated and coupled. In the multilayer film with $n=2$, the SPs are gradually generated on the four interfaces of silver-SiO_2 and are strongly coupled [as shown in Figs. 9(A1)–9(A6)]. By increasing n, the coupling of electromagnetic wave happens in the entire multilayer film [as shown in Figs. 9(B1)–9(B6) and 9(C1)–9(C6)]. Electromagnetic waves can be coupled on two interfaces of one silver layer [as shown in Fig. 9(A3)], or among the four interfaces of two silver layers [as shown in Figs. 9(A4), 9(B2), and 9(C2)], or even among a number of interfaces of several silver layers [as shown in Figs. 9(B3)–9(B6) and 9(C3)–9(C6)]. Consequently, the coupling of SPs is a collective effect and plays an important role in the enhancement of optical transmission in the multilayers.

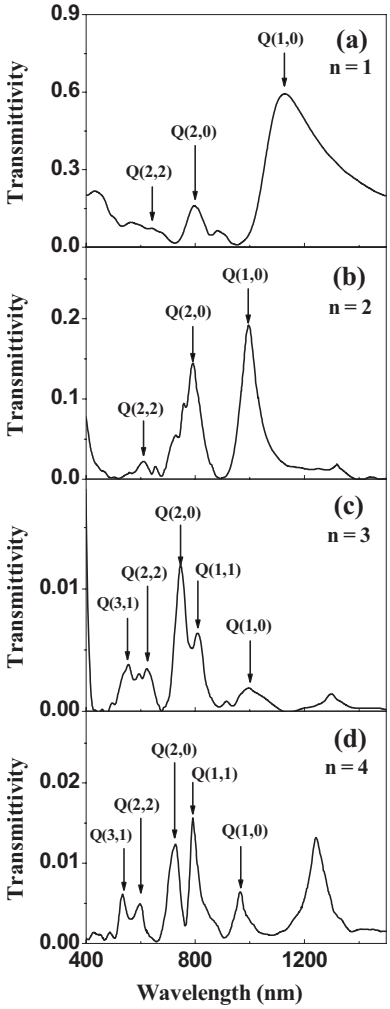

FIG. 10. The measured transmittivity of the nanostructured Ag/SiO_2 multilayer films described in Fig. 8. The repeating numbers of building blocks are (a) $n=1$, (b) $n=2$, (c) $n=3$, and (d) $n=4$, respectively. Here, the incident beam is perpendicular to the film.

Experimentally, the above discussed nanostructured Ag/SiO_2 multilayer films have been fabricated by magnetron sputtering and FIB facility. In the measured transmission spectra, several peaks were observed in the visible and near-infrared ranges, as shown in Figs. 10(a)–10(d). The major peaks can be indexed by two integers based on the effective permittivity. By increasing the number of building blocks, the quality factor of the peak increases. For example, the peak labeled by $Q(2,0)$ has the quality factor $Q=10.0$ for $n=1$, but $Q=15.1$ for $n=4$. Yet due to the absorption of silver, the intensity of transmission peak significantly decreases when n increases. Two new resonant modes labeled by $Q(3,1)$ and $Q(1,1)$ gradually enhance and finally become distinct in the multilayer film containing four building blocks [as shown in Fig. 10(d)]. We suggest that the new resonant mode originates from the coupling of SPs in the nanostructured Ag/SiO_2 multilayer films. In our multilayer films, $Ag\text{-}SiO_2$ interface is the only type of interface. Therefore, the resonant modes come from both the SPs on the $Ag\text{-}SiO_2$ interface and the coupling of SPs. The coupling of SPs strongly depends on the structure of multilayer, which makes it possible to adjust the number of transmission modes, the location and quality factor of the mode, and so on. These features can be applied to tune electromagnetic wave in subwavelength optoelectronic devices.

The experimental result agrees reasonably well with the calculated one. The deviation between the experimental and the calculated results might arise from inhomogeneity of the samples. The other possibility could be that in measuring the transmission spectra experimentally, we only pick up the diffraction around the zeroth order, and the higher order of diffraction off the normal direction will not be collected. In the FDTD calculation, however, a surface integral of all the flux is used, which includes not only zeroth-order normal to the plane but also the higher order of diffraction as well.

IV. SUMMARY

To summarize, we demonstrate in this paper that the transmission optical enhancement originates not only from the surface plasmons (SPs) but also from the coupling of SPs in the Ag/SiO_2 multilayer with a periodic array of subwavelength holes. The coupled SPs in the nanostructured Ag/SiO_2 multilayer film can be characterized using an effective-permittivity model. The resonant modes in the transmission spectra can be analytically indexed. The optical measurements are in good agreement with the numerical calculations based on FDTD method. It is found that the coupling of SPs strongly depends on the detailed structure of the film. In the sandwich centered with a structured silver film, the coupling of SPs leads to the shift of transmission peaks, which enlarges when the thickness of the silver film is decreased. In the nanostructured Ag/SiO_2 multilayer, where the silver film is perforated with an array of subwavelength holes, the coupling of SPs can yield a new resonant mode, and the quality factor of the transmission peaks increases when the number of building blocks is increased. Physically, these features originate from multiple scatterings and the coupling of electromagnetic waves on the interfaces of the multilayers. We suggest that these properties may have potential applications in subwavelength optoelectronic devices.

ACKNOWLEDGMENTS

This work was supported by the grants from the National Natural Science Foundation of China 10625417, 50672035, and 90601001, the State Key Program for Basic Research from the Ministry of Science and Technology of China (2004CB619005 and 2006CB921804), and partly by the Ministry of Education of China (NCET-05-0440).

*Author to whom correspondence should be addressed; rwpeng@nju.edu.cn

[1] R. H. Ritchie, Phys. Rev. **106**, 874 (1957).
[2] T. W. Ebbesen, H. J. Lezec, H. F. Ghaemi, T. Thio, and P. A. Wolff, Nature (London) **391**, 667 (1998).
[3] L. Martín-Moreno, F. J. García-Vidal, H. J. Lezec, K. M. Pellerin, T. Thio, J. B. Pendry, and T. W. Ebbesen, Phys. Rev. Lett. **86**, 1114 (2001).
[4] C. Genet and T. W. Ebbesen, Nature (London) **445**, 39 (2007).
[5] I. Avrutsky, Y. Zhao, and V. Kochergin, Opt. Lett. **25**, 595 (2000).
[6] D. E. Grupp, H. J. Lezec, T. W. Ebbesen, K. M. Pellerin, and T. Thio, Appl. Phys. Lett. **77**, 1569 (2000).
[7] T. Thio, H. F. Ghaemi, H. J. Lezec, P. A. Wolff, and T. W. Ebbesen, J. Opt. Soc. Am. B **16**, 1743 (1999).
[8] A. Degiron, H. J. Lezec, W. Barnes, and T. Ebbesen, Appl. Phys. Lett. **81**, 4327 (2002).
[9] K. L. van der Molen, F. B. Segerink, N. F. van Hulst, and L. Kuipers, Appl. Phys. Lett. **85**, 4316 (2004); Y. J. Bao, B. Zhang, J. W. Si, Mu Wang, R. W. Peng, X. Lu, J. Shao, Z. F. Li, X. P. Hao, and N. B. Ming, *ibid.* **90**, 251914 (2007).
[10] K. J. Klein Koerkamp, S. Enoch, F. B. Segerink, N. F. van Hulst, and L. Kuipers, Phys. Rev. Lett. **92**, 183901 (2004); K. L. van der Molen, K. J. Klein Koerkamp, S. Enoch, F. B. Segerink, N. F. van Hulst, and L. Kuipers, Phys. Rev. B **72**, 045421 (2005).
[11] Wenjun Fan, Shuang Zhang, Babar Minhas, Kevin J. Malloy, and S. R. J. Brueck, Phys. Rev. Lett. **94**, 033903 (2005).
[12] William L. Barnes, Alain Dereux, and Thomas W. Ebbesen, Nature (London) **424**, 824 (2003).
[13] J. B. Pendry, Phys. Rev. Lett. **85**, 3966 (2000); D. R. Smith, W. J. Padilla, D. C. Vier, S. C. Nemat-Nasser, and S. Schultz, *ibid.* **84**, 4184 (2000); R. A. Shelby, D. R. Smith, S. C. Nemat-Nasser, and S. Schultz, Appl. Phys. Lett. **78**, 489 (2001).
[14] D. R. Smith, J. B. Pendry, and M. C. K. Wiltshire, Science **304**, 788 (2004).
[15] N. Fang, H. Lee, C. Sun, and X. Zhang, Science **308**, 534 (2005); Z. Liu, H. Lee, Y. Xiong, C. Sun, and X. Zhang, *ibid.* **315**, 1686 (2007).
[16] E. Ozbay, Science **311**, 189 (2006).
[17] A. Krishnan, T. Thio, T. J. Kim, H. J. Lezec, T. W. Ebbesen, P. A. Wolff, J. Pendry, L. Martin-Moreno, and F. J. Garcia-Vidal, Opt. Commun. **200**, 1 (2001); Y. H. Ye and J. Y. Zhang, Opt. Lett. **30**, 1521 (2005).
[18] A. Taflove and S. C. Hagness, *Computational Electrodynamics: The Finite-Difference Time-Domain Method*, 3rd ed. (Artech House, Norwood, 2005).
[19] A. D. Rakic, A. B. Djurisic, J. M. Elazar, and Marian L. Majewski, Appl. Opt. **37**, 5271 (1998).
[20] N. Stefanou, A. Modinos, and V. Yannopapas, Solid State Commun. **118**, 69 (2001).
[21] J. C. Maxwell-Garnett, Philos. Trans. R. Soc. London, Ser. A **203**, 385 (1904).
[22] U. Fano, Phys. Rev. **124**, 1866 (1961); G. Gantzounis and N. Stefanou, Phys. Rev. B **72**, 075107 (2005).
[23] C. Genet, M. P. van Exter, and J. P. Woerdman, Opt. Commun. **225**, 331 (2003).